All fiber tunable- or dual-wavelength Yb-doped fiber laser covering from dissipative soliton to dissipative soliton resonance

Zhaokun Wang (王兆坤)[1,2], Songtao Du (杜松涛)[1], Jianhua Wang (王建华)[3], Feng Zou (邹 峰)[1,2], Ziwei Wang (王子薇)[1,2], Wendi Wu (吴闻迪)[1], and Jun Zhou (周 军)[2,*]

[1]*Shanghai Key Laboratory of Solid State Laser and Application, and Shanghai Institute of Optics and Fine Mechanics, Chinese Academy of Sciences, Shanghai 201800, China*

[2]*Graduate University of the Chinese Academy of Sciences, Beijing 100049, China*

[3]*Department of Space and Command, Academy of Equipment, Beijing 101416, China*

**Corresponding author: junzhousd@mail.siom.ac.cn*

Received November 26, 2015; accepted February 4, 2016; posted online March 28, 2016

In this Letter, a simple and passively mode-locking Yb-doped all fiber laser using a nonlinear polarization rotation technique operating under dissipative soliton (DS) or dissipative soliton resonance (DSR) conditions is proposed. Furthermore, using a combination of a bandpass filter and a Loyt filter, tunable single-wavelength or dual-wavelength operation under two different conditions is realized, respectively. The tunable single-wavelength DS laser has a 5 nm tuning range from 1029 to 1034 nm with a pulse width of 110 ps. The tunable single-wavelength DSR operation laser has a range of 4 nm. In-depth research on the mechanism of the conversion between DS and DSR is carried out. Particularly, under dual-wavelength DSR operation, the obtained step-like pulses consist of two rectangular pulses with different energies. This work could help give a deeper insight into normal dispersion pulses.

OCIS codes: 320.7090, 140.3615, 140.3600, 140.4050.
doi: 10.3788/COL201614.041401.

In recent years, passively mode-locked Yb-doped fiber lasers (YDFLs) operating in a normal dispersion regime have attracted increasing attention because of their compactness, low cost, and widespread applications in material processing and fiber sensing[1]. Since the dispersion is shifted to the normal regime, researchers obtain dissipative soliton (DS) generation. Generally, the spectrum has a typical steep edge due to the filter effect. However, the pulse energy is easily limited to ~20 nJ due to the multi-pulsing instability phenomenon[2]. In order to improve the pulse energy scaling ability, other pulse formation mechanisms and dynamics should be researched. Recently, a soliton formation mechanism called dissipative soliton resonance (DSR) was theoretically proposed to achieve a pulse through selecting proper parameters in the frame of the complex Ginzburg–Landau equation[3,4]. According to the model under the DSR condition, the pulse formed could increase its energy and width indefinitely with increasing pump power. Meanwhile, pulse amplitude remains constant with a rectangular shape. The experimental observations confirmed that the DSR phenomenon could indeed exist in fiber lasers either in anomalous dispersion or in normal dispersion regimes of lasers. The rectangular pulses' effect was observed experimentally in an Er-doped all-normal-dispersion laser cavity for the first time[5]. Dual-wavelength step-like pulses consisting of two rectangular pulses with different energies were delivered from an Er-doped fiber laser[6]. Indeed, the rectangular pulse could be experimentally obtained despite the dispersion regime and gain medium, even in all-normal-dispersion YDFLs[7–10]. Around 1 μm, the pulse-width-tunable nanosecond flat-top pulses were observed in a self-started passively mode-locked fiber laser[7]. As mentioned above, most experimental research to date has only focused on either DS or DSR. It is theoretically indicated that DS and DSR can be realized in one and the same mode-locked fiber laser[11]. However, to the best of our knowledge, no experimental observation of the DS and DSR in one and the same YDFL has been reported.

In addition, several passively mode-locked methods for achieving wavelength-tunable or dual-wavelength operation have been achieved, including semiconductor saturable absorption mirrors[12], carbon nanotubes[13], graphene oxide[14,15], topological insulator saturable absorbers (SAs)[16], and nonlinear polarization rotation (NPR) mechanisms[17,18]. Based on a birefringent filter, wavelength tunability for both single- and dual-wavelength DS mode-locking lasers has been attained[19]. Zhang *et al.* have reported a tunable single-wavelength Er-doped fiber laser by using atomic layer graphene[20]. Among these approaches, the most popular one used to realize the tunable operation of fiber lasers is to incorporate an additional tunable comb filter, such as the Lyot filter, constructed by a section of polarization-maintaining fiber (PMF)[19,21]. So far, the reported output rectangular pulses usually operated at a fixed wavelength. In some applications, fiber

lasers that generate dual- or multi-wavelength pulses would be more favorable. It should be mentioned that the wavelength-tunable or multi-wavelength DSR delivering around 1 μm needs to be further investigated.

In this Letter, we demonstrate a simple, compact, and passively mode-locking YDFL using the NPR technique covering from DS to DSR operation. The pulse duration of the DS is fixed at about 110 ps, while that of the DSR is tuned from 6.3 to 74.8 ns with increasing power. Through the introduction of the Loyt filter, the tunable single-wavelength and dual-wavelength mode-locking operations under two different conditions are both realized. The tuning range of DS and DSR is about 5 and 4 nm, respectively. In particular, the step-like pulses under dual-wavelength DSR operation consisting of two different rectangular pulses with different energies are observed. To the best of our knowledge, this is the first time that the tunable characteristic of DS and DSR operation is simultaneously observed in the same cavity and the phenomenon of dual-wavelength DSR has the output of a step-like pulse around 1 μm. The demonstrated fiber laser delivers flexible pulse output, and the experiment indicates that the combination of the bandpass filter and the laser plays an important role in the formation of this flexible operation. Our work might produce some innovative applications for related fields and also help gain a deeper insight of normal dispersion pulses.

The laser setup is illustrated in Fig. 1. The ring cavity is made of pure normal dispersion fibers. The 600 mW single-mode pigtailed laser diode emitting at 976 nm is coupled into the cavity through a 976/1030 fiber pigtailed multiplexer. A piece of 1-m-long highly Yb-doped single-mode fiber with nominal core absorption of more than 250 dB/m at 976 nm is used as a gain medium. A polarization-maintaining (PM) isolator with its fast axis blocked is inserted between the two polarization controllers (PCs), which act as an equivalent SA. In addition, two PCs, together with a section of 77-cm-long PMF after the isolator with an angle of 45°, are utilized to generate an equivalent Lyot birefringence fiber filter[22]. The corresponding periodic filter bandwidth is 3.4 nm. The bandwidth $\Delta\lambda$ is decided by the formula $\lambda^2/(\Delta n \cdot L)$, where λ is the central wavelength, L is the length of the PM fiber, and $\Delta n = n_{\text{slow}} - n_{\text{fast}}$ is the strength of birefringence. Approximately 20% of the beam is extracted from the cavity through a fiber coupler. A bandwidth filter with a central wavelength of 1030 nm and 3 dB bandwidth of ~8 nm is inserted into the cavity to suppress the mode competition effect. The overall fiber length of the laser cavity and the estimated total dispersion of the laser cavity are 750 m and 18 ps^2 at 1030 nm, respectively.

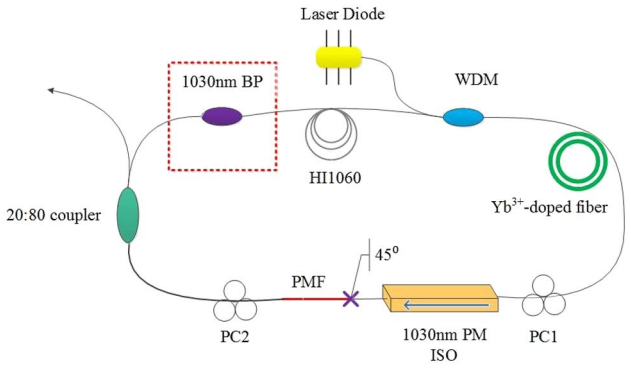

Fig. 1. Schematic of the experimental setup. WDM, wavelength division multiplexer; BP, bandpass filter.

The output laser is detected by an optical spectrum analyzer (Yokogawa AQ6370B) and a 6 GHz digital storage oscilloscope together with an 11 GHz photodetector. The pulse duration is measured by an autocorrelator (APE Pulse Check).

The self-started passive mode-locking operation is realized based on the NPR technique composed of the PM isolator and PCs. Due to the multi-wavelength filtering effect introduced by the combination of Loyt and bandpass filters, different laser operations could be observed, including tunable single-wavelength, dual-wavelength DS, tunable single-wavelength, and dual-wavelength DSR operation.

In the experiment, the mode-locking state of single-wavelength lasing DS and DSR operation can be realized by properly rotating the PCs. Figure 2 shows the characteristics of a typical single-wavelength DS and DSR operation. The conventional DS with steep spectral edges could be obtained as the pump power was increased

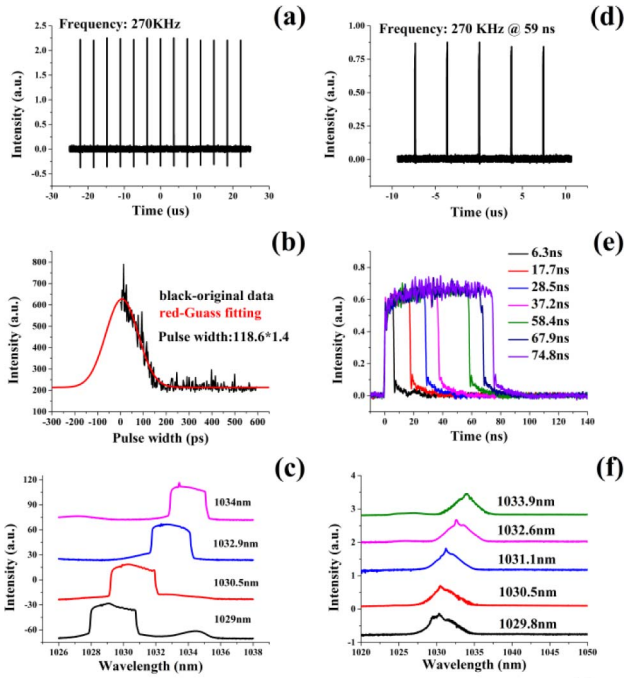

Fig. 2. Single-wavelength operation under DS condition output: (a) mode-locking pulse train, (b) the corresponding pulse width, (c) tunability of output spectra. Single-wavelength operation under DSR condition output: (d) pulse train operating in DSR region at a pump power of 192 mW, (e) rectangular pulses of the mode-locked fiber laser under different pump power, (f) tunability of single-wavelength DSR operation.

above the threshold of ~45 mW. A stable pulse train at a fundamental repetition rate of 270 kHz that matches well with the cavity length was observed, as shown in Fig. 2(a). The average output power is about ~0.8 mW with a pump power of 60 mW corresponding to the single-pulse energy of ~2.96 nJ. Figure 2(b) shows the autocorrelation of the pulse width. Assuming a Gaussian pulse profile, the pulse duration is 118.6 ps. The time–bandwidth product is 77.9, indicating that the pulses have a large chirp. The large chirp of the DS can be attributed to the combination of normal dispersion and fiber nonlinearity. Due to the pump hysteresis phenomenon, the fiber laser could maintain the mode-locking state when the pump power is decreased[23,24]. Owing to the tunable characteristic of the Loyt filter, the lasing wavelength of the single-wavelength mode-locked DS can be continuously tuned just through adjusting the PC. As shown in Fig. 2(c), under different settings of PCs, the center wavelengths located at 1029, 1030.5, 1032.9, and 1034 nm are obtained. The center wavelength of the pulses could be tuned from 1029 to 1034 nm in a range of 5 nm. During the whole tuning range, the spectra retain the steep edges, and the spectral bandwidths of the pulses are not remarkably different from the edge-to-edge spectral bandwidth of 2.5 nm.

As we know, in the NPR-based fiber ring laser, the pump level, cavity loss, and spectral filtering introduced by the PC play an important role in the formation of pulse dynamics[3,25]. Therefore, different types of pulse formations could be achieved by changing these parameters. By further increasing the pump power, the pulse breaks free, the pulse width and the pulse energy increase approximately linearly with the increasing pump power, while the peak power of the pulse remains almost constant. Also, the pulse profile retains its rectangular shape. This is the typical signature of the DSR phenomenon. The repetition rate is 270 kHz as determined by the cavity length. Figure 2(d) shows the corresponding pulse train with a large scan range. The corresponding evolution of the pulse as a function of the pump power is shown in Fig. 2(e). The pulse widths are tunable from 6.3 to 74.8 ns when the pump power increases from 62 to 251 mW. In this case, the maximum output power and pulse energy are 13 mW and 48 nJ, respectively, which is limited by the pump power level. Under the DSR condition, due to the Loyt filter, the lasing wavelength of the single-wavelength DSR could also be continuously tuned within the range of 4 nm from 1029.8 to 1033.9 nm. Typical output laser spectra at the pump power of 156 mW are shown in Fig. 2(f). It is worth noting that the 3 dB bandwidth of the mode-locked spectrum is almost constant at ~0.6 nm as the center wavelength is tuned.

It is apparent that the fiber laser could achieve switchable DS and DSR mode locking by tuning the PC under appropriate tuning of the pump. Figure 3 shows the evolution of the pulse versus launched pump power. At low pump power, the laser mode-locks and generates DS pulses, and the DS then begin to experience multipulsing. As the launched pump power increases, DSR begins to

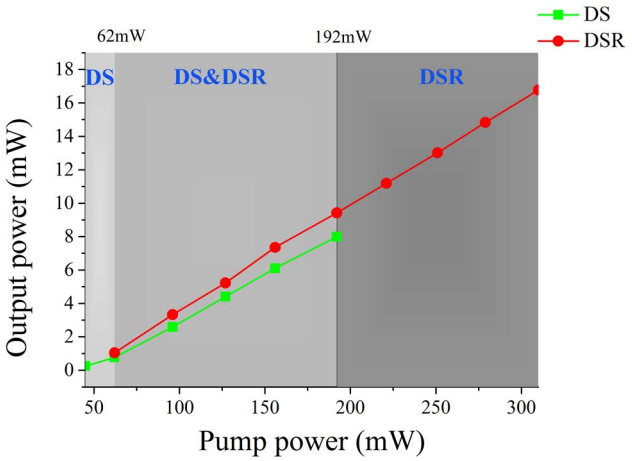

Fig. 3. Oscillator output power versus launched pump power.

appear. At ~200 mW, DS pulses no longer exist. In the normal dispersion regime, the reserve saturable absorption plays a key role in generating DSR pulses. The reserve saturable absorption stands for a phenomenon where the transmissivity decreases with increasing instantaneous power. Most DSR phenomenon were reported based on NPR and the nonlinear loop mirror, as the SA exhibits a nonlinear transmission of a sinusoid curve. As a result, we believe that at a comparatively low pump power, the peak power doesn't reach into the reverse saturable absorption power range, the cavity delivers DS, the pulse energy and peak power increase with the pump power increasing in this regime, and the bandwidth of the spectrum broadens due to the strong nonlinear effect introduced. Next, the peak power is high enough, the reverse saturable absorption is activated, and higher instantaneous power would experience larger loss, which brings the pulse evolving horizontally instead of vertically[11]. Also, in this condition, the linear chirp is very small so the pulse is hard to suppress. The DSR operation is an efficient way to improve the pulse energy's scaling ability. It should be noted that at the pump power from ~60 to ~192 mW, both DS and DSR could operate by adjusting PCs. We attribute it to the variation in the switching intensity level of the sinusoid curve, which is sensitive to perturbation induced by simply tuning PCs. As a result, the threshold of generating a DSR pulse would be influenced by tuning PCs.

In the experiment, to verify whether the combination of the bandpass filter and the Loyt birefringence fiber filter are contributing to the tunable DS and DSR operation, the bandpass filter and the 77 cm length of PM fiber are removed from the cavity, respectively. When the bandpass filter is removed, only the tunable single-, dual-, and multi-wavelength DS could be achieved. In this case, the polarization-tunable characteristic of the Loyt filter results in the tuning multi-wavelength operation. Without bandpass restrictions on the wavelength, a wider tuning range could be obtained When the bandpass filter is left in the cavity, only the DSR operation could be observed, while the wavelength tunable operation could not

be achieved anymore. By this comparison, we consider that the flexible operation is mostly attributed to the combination of the Loyt filter and the bandpass filter. However, the mechanism needs to be further investigated.

Taking advantage of the comb filter effect of the Loyt filter, the dual-wavelength mode-locking operation can also be obtained from the fiber laser as the pump power is fixed. Figure 4 describes the output characteristics of a typical dual-wavelength mode-locking state obtained under 62 mW pump power. Figure 4(a) shows the spectrum on a logarithmic scale. The 3 dB spectral bandwidths of the two separated steep-edge spectra at the center of 1026.4 and 1034.7 nm are both ~2 nm. Due to the effect of mode competition, the bandwidths of the two separated mode-locked pulse spectra are narrower than those under the single-wavelength DS condition. Figure 4(b) shows the synchronous oscilloscope trace of the dual-wavelength DSs. There are two DSs propagating with different group velocities in the cavity. Therefore, the two pulse trains will distribute randomly on the oscilloscope. When the pump power is increased to 87 mW, one of the pulses first breaks up into bursts one by one, while the other remains the same. Upon increasing the pump power, two bursts of multiple pulses appear. In addition, this phenomenon is reversible by decreasing the pump power such that the operation converted into single-wavelength operation centered at 1026.4 nm with CW operation at 1034.7 nm next to two CWs in operation. It could be proved that the

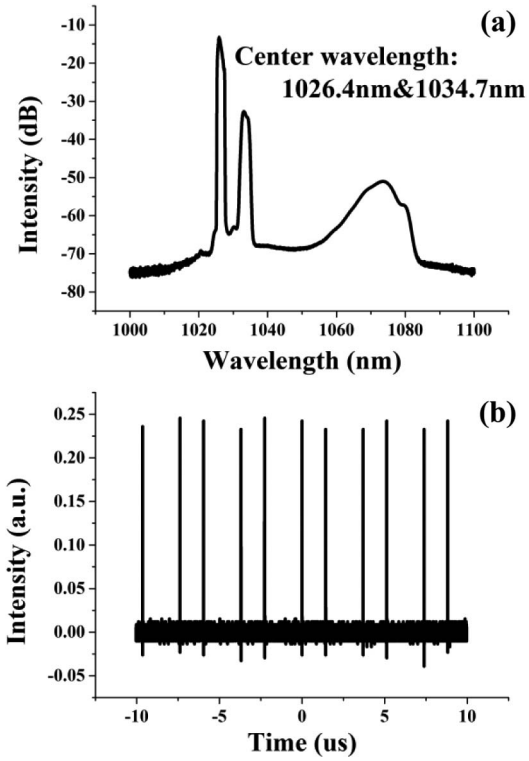

Fig. 4. Dual-wavelength DS output: (a) spectrum on logarithmic scale, (b) corresponding mode-locking pulse train with pump power of 62 mW.

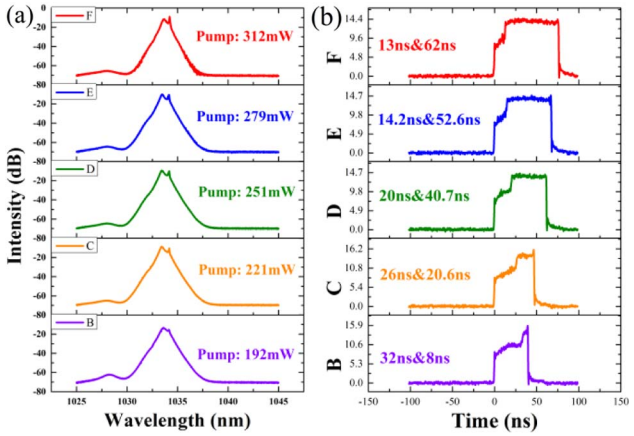

Fig. 5. (a) Optical spectrum of dual-wavelength DSR operation with different pump power, and (b) corresponding step-like pulse.

dual-wavelength DS operation evolved from the operation of two CWs.

In particular, a dual-wavelength step-like pulse has also been achieved by adjusting PCs. Figure 5(a) presents the typical dual-wavelength spectrum of the step-like pulse with increasing pump power. As can be seen from Fig. 5(a), the dual wavelength oscillates at the center of 1033.4 and 1034.1 nm. The fundamental cavity repetition is about 270 kHz, which is in good agreement with the cavity length. The wavelength centered at 1034.1 nm gradually strengthens with the increasing pump power. This evolution of step-like pulses in the spectral domain is consistent with that in temporal domain. As could be seen in Fig. 5(b), the pulse directly from the cavity exhibits step-like profiles. The whole step-like pulse width broadens linearly with pump power increasing, while the weaker pulse narrows from 32 to 13 ns, and the pulse with higher intensity broadens from 8 to 62 ns. In the experiment, the dynamics of the dual-wavelength DSR evolution with the varying pump power is investigated. The stronger pulses could undergo much higher gain as the pump power increases and finally suppress the energy of the weaker pulse, presented in Fig. 5(b). It can be clearly seen that the wavelength centered at 1033.4 and 1034.1 nm in the spectral domain corresponds to the stronger and the weaker pulse, respectively. It is apparent that the peak power of the two pulses keeps almost constant, which is the significant feature of the DSR operation. Also, the two rectangular pulse at different wavelengths always adhere to each other. In addition, this phenomenon is induced mainly by the balance of large dispersion and nonlinearity. In a normal dispersion regime, propagating pulses centered at 1034.1 nm travel faster than the pulses centered at 1033.4 nm. However, a different pulse intensity introduced the variation of the nonlinear refractive index, and the strong pulse centered at 1033.4 nm would experience higher nonlinearity and larger refractive index. Ultimately, two rectangular pulses of different intensity propagate in a formation of step-like pulses. Based on

the experiment, it could be concluded that the fiber laser works at stable dual-wavelength mode-locked operation.

The step-like pulses consisted of two rectangular pulses with different energies that are quite different from the other dual-wavelength mode-locking pulses holding the same property such as conventional multisolitons[26] or bound-state solitons[27]. The comb filter caused by the Loyt filter eventually leads to the formation of dual wavelengths. When the PCs are in a proper state, the wavelength centered at 1033.4 and 1034.1 nm could experience quite low loss, while other wavelengths are suppressed. Finally, dual-wavelength mode-locking operation with each center wavelength corresponding to an independent rectangular pulse is achieved. In addition, due to the reserve saturable absorption, the output pulse exhibits nanosecond duration and a rectangular profile with a flat top[6]. The obtained results reveal an operational regime of multi-wavelength pulses for square profiles in a fiber laser.

In conclusion, we demonstrate for the first time to our knowledge an all-normal-dispersion YDFL delivering flexible output, including tunable single-wavelength, dual-wavelength DS, tunable single-wavelength, and dual-wavelength DSR operation based on a birefringence fiber filter. As a result, the tunable single-wavelength DSs have a 5 nm tuning range from 1029 to 1034 nm. The formation dynamics of tunable single-wavelength DSR operation with a range of 4 nm are obtained. The output pulse duration changes from 6.3 to 74.8 ns with increasing pump power. The phenomenon of dual-wavelength DS and DSR operation can be observed at the same time. In particular, under dual-wavelength operation, the step-like pulses obtained consist of two rectangular pulses with different energies. It is found that the switching of different operations is mainly determined by the NPR effect and the different enhanced self-amplitude modulation effect through spectral filtering. Such an all fiber simple and compact laser with lasing wavelength tunability and flexibility has great potential for the previously mentioned applications.

This work was supported in part by the National High Technology Research and Development Program of China (No. 2014AA041901), the NSAF Foundation of National Natural Science Foundation of China (No. U1330134), the project of Shandong Province Higher Educational Science and Technology Program (No. J13LJ06), the National Natural Science Foundation of China (No. 61308024), and the National Natural Science Fund (No. 11174305).

References

1. P. Grelu and N. N. Akhmediev, Nat. Photon. **6**, 84 (2012).
2. A. Chong, W. H. Renninger, and F. W. Wise, Opt. Lett. **32**, 2408 (2007).
3. W. Chang, A. Ankiewicz, J. M. Soto-Crespo, and N. Akhmediev, Phys. Rev. A **78**, 023830 (2008).
4. W. Chang, J. M. Soto-Crespo, A. Ankiewicz, and N. Akhmediev, Phys. Rev. A **79**, 033840 (2009).
5. X. Wu, D. Y. Tang, H. Zhang, and L. M. Zhao, Opt. Express **17**, 5580 (2009).
6. D. Mao, X. Liu, L. Wang, H. Lu, and L. Duan, Opt. Express **19**, 3996 (2011).
7. W. Li, Q. Hao, M. Yan, and H. Zeng, Opt. Express **17**, 10113 (2009).
8. N. Zhao, M. Liu, H. Liu, X. Zheng, Q. Ning, A. Luo, Z. Luo, and W. Xu, Opt. Express **22**, 10906 (2014).
9. K. Özgören, B. Öktem, S. Yilmaz, F. Ö. Ilday, and K. Eken, Opt. Express **19**, 17647 (2011).
10. L. Liu, J. Liao, Q. Ning, Y. Wei, A. Luo, S. Xu, Z. Luo, Z. Yang, and W. Xu, Opt. Express **21**, 27087 (2013).
11. Z. Cheng, H. Li, and P. Wang, Opt. Express **23**, 5972 (2015).
12. Z. Luo, A. Luo, and W. Xu, IEEE Photon. J. **3**, 64 (2011).
13. X. Li, Y. Wang, Y. Wang, X. Hu, W. Zhao, X. Liu, J. Yu, C. Gao, W. Zhang, and Z. Yang, IEEE Photon. J. **4**, 234 (2012).
14. S. Huang, Y. Wang, P. Yan, J. Zhao, H. Li, and R. Lin, Opt. Express **22**, 11417 (2014).
15. L. Zhang, Z. Zhuo, R. Wei, Y. Wang, X. Chen, and X. Xu, Chin. Opt. Lett. **12**, 021405 (2014).
16. B. Guo, Y. Yao, Y. F. Yang, Y. J. Yuan, L. Jin, B. Yan, and J. Y. Zhang, Photon. Res. **3**, 94 (2015).
17. Z. X. Zhang, Z. W. Xu, and L. Zhang, Opt. Express **20**, 26736 (2012).
18. L. Zhang, J. Hu, J. Wang, and Y. Feng, Opt. Lett. **37**, 3828 (2012).
19. Z. X. Zhang, Z. W. Xu, and L. Zhang, Opt. Express **20**, 26736 (2012).
20. H. Zhang, D. Y. Tang, L. M. Zhao, Q. L. Bao, K. P. Loh, B. Lin, and S. C. Tjin, Laser Phys. Lett. **7**, 591 (2010).
21. Z. W. Xu and Z. X. Zhang, Laser Phys. Lett. **10**, 085105 (2013).
22. K. Özgören and F. Ö. Ilday, Opt. Lett. **35**, 1296 (2010).
23. X. Li, S. Zhang, Y. Hao, and Z. Yang, Opt. Express **22**, 6699 (2014).
24. X. M. Liu, Phys. Rev. A **81**, 023811 (2010).
25. E. Ding, P. H. Grelu, and J. N. Kutz, Opt. Lett. **36**, 1146 (2011).
26. L. E. Nelson, D. J. Jones, K. Tamura, H. A. Haus, and E. P. Ippen, Appl. Phys. B **65**, 277 (1997).
27. N. N. Akhmediev, A. Ankiewicz, and J. M. Soto-Crespo, J. Opt. Soc. Am. B **15**, 515 (1998).